

Generalized antireflection coatings for complex bulk metamaterials

Ruben Maas,^{1,*} Sander A. Mann,^{1,*} Dimitrios L. Sounas,² Andrea Alù,^{1,2} Erik C. Garnett,¹ and Albert Polman^{1,†}

¹Center for Nanophotonics, FOM Institute AMOLF, Science Park 104, 1098 XG Amsterdam, The Netherlands

²Department of Electrical and Computer Engineering, The University of Texas at Austin, 1616 Guadalupe St., Austin, Texas 78701, USA

(Received 20 December 2015; revised manuscript received 30 March 2016; published 24 May 2016)

We present the optimized design of an antireflection coating to efficiently couple an incident plane wave into a metamaterial with a complex field profile. We show that such an antireflection coating must enable spatial engineering of the field profiles at the coating/metamaterial interface to achieve high transmission, and therefore it is required to be inhomogeneous. As a demonstration, we investigate theoretically a waveguide-based negative-index metamaterial, which under normal incidence cannot be excited due to the antisymmetric propagating eigenmode. Through careful engineering of the field profile, lateral position, and thickness of the coating layer, we enhance the transmission under normal incidence from 0% to 100%. This principle may generally be applied to overcome low coupling efficiency between incident plane waves and complex mode profiles in metamaterials.

DOI: [10.1103/PhysRevB.93.195433](https://doi.org/10.1103/PhysRevB.93.195433)

I. INTRODUCTION

Optical metamaterials, structures of which the effective properties are derived from subwavelength elements, have recently attracted a lot of attention [1,2]. Metamaterials can be used to achieve hyperbolic dispersion [3–7], epsilon-near-zero response [8], or an effective negative index response [9–12]. While the effective optical properties of these metamaterials can be very interesting, the excitation of such media is often quite poor. This is a direct result of the fact that the propagating eigenmodes of such bulk metamaterials can have complex field profiles, which are not excited efficiently by simple plane waves. In this paper, for instance, we focus on the interesting optical properties that arise from antisymmetric eigenmodes supported by waveguide metamaterials. These antisymmetric waveguide modes may support a negative refractive index [13], which can, for example, be utilized to realize a flat lens but cannot be excited from free space under normal incidence due to their asymmetry.

To enhance transmission into bulk media, many optical systems use antireflection coatings, which lead to reflection cancellation through destructive interference between the reflected light from the air-coating and coating-medium interfaces. However, the simple homogeneous antireflection coatings that are used in conventional optical systems cannot solve the spatial field mismatch between plane waves and antisymmetric metamaterial eigenmodes: In the homogeneous coating, the incident field profile is still symmetric.

Here, we propose structuring the coating layer to achieve very large coupling into complex bulk metamaterials. The use of nanoscale structures to enhance transmission into homogeneous media has been demonstrated before [14–17]. Aside from impedance matching, we simultaneously utilize the more complicated field profiles in such a nanostructured antireflection coating to achieve significant field overlap with the substrate eigenmodes of interest, enabling perfect transmission even for an extreme mismatch between the

incident wave and the substrate eigenmodes, as in the case of a plane wave coupling to antisymmetric modes.

II. EXCITATION OF METAMATERIAL WAVEGUIDE MODES

The proposed approach is demonstrated in the case of a multilayer stack formed by metal and dielectric thin films. There has been a lot of interest in light propagation through such multilayer geometries [18–23]. For example, a metal/air grating was first considered to explain the observed phenomenon of extraordinary optical transmission [24,25]. The special dispersive characteristics of these multilayer metamaterials are due to coupled surface plasmon polaritons that propagate along the metal/dielectric waveguide interfaces. Furthermore, multilayer structures allow the derivation of analytical formulas for their eigenmodes and in several cases for their transmission and reflection properties as well.

Figure 1(a) shows a sketch of the geometry under consideration. Our metamaterial is formed by a periodic array of thin metallic layers (with thickness d_m and permittivity ε_m) and thin dielectric layers (with thickness d_d and permittivity ε_d), with unit cell size $a = d_m + d_d$. We take the direction of periodicity as the \hat{x} direction, and $x = 0$ to coincide with the center of the dielectric layer of the unit cell. The waveguides are infinitely extended in the \hat{y} direction, and interfaces between different regions are normal to \hat{z} .

For our demonstration, we investigate a lossless configuration, which has a single propagating mode with an antisymmetric profile and a negative mode index: $\beta_1^{(2)} = -28.9 \mu\text{m}^{-1}$. Following the sketch in Fig. 1(a), the parameters of the structure are $d_m = 45 \text{ nm}$, $\varepsilon_m = -3.5$, $d_d = 20 \text{ nm}$, and $\varepsilon_d = 6.25$ for $\lambda_0 = 450 \text{ nm}$. All other modes supported by the metamaterial are either evanescent or anomalous [22,26]. Figure 1(b) shows the field profile of the negative index mode, confirming the odd symmetry with respect to the dielectric core. We denote the field by $h_y(x)$ to differentiate the waveguide mode field profile from the total magnetic field $H(x, z)$, which is the sum of all incident, reflected, and transmitted modes. Figure 1(c) shows the total magnetic field distribution near the interface when the multilayer structure is illuminated with an incident plane wave at normal incidence,

*These authors contributed equally to the work.

†polman@amolf.nl

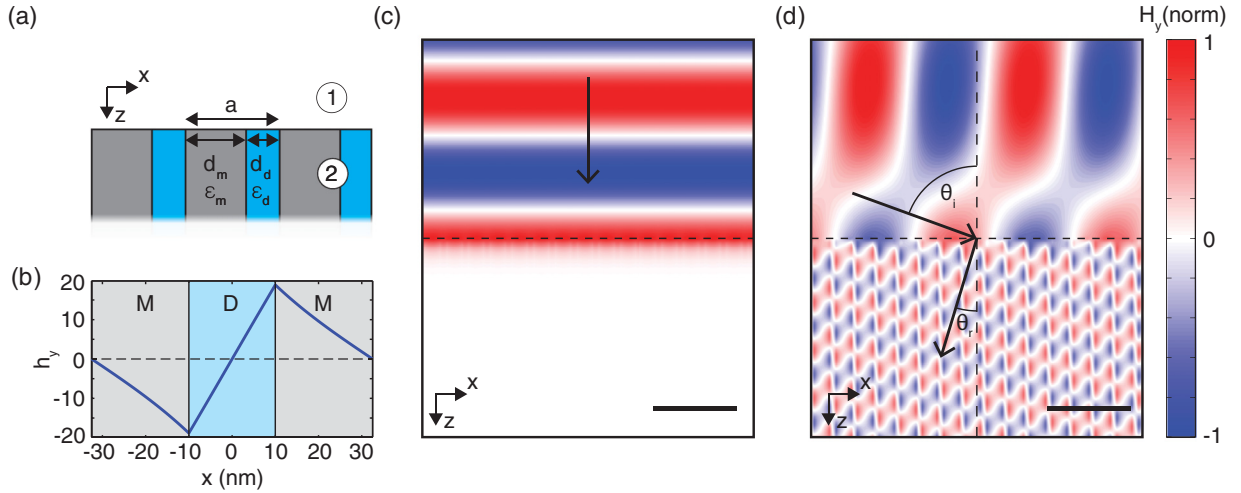


FIG. 1. (a) Sketch of metal-dielectric metamaterial geometry. (b) The negative-index waveguide mode field profile $h_y(x)$ ($d_m = 45$ nm, $\epsilon_m = -3.5$, $d_d = 20$ nm, $\epsilon_d = 6.25$, and $\lambda_0 = 450$ nm). The field profile is antisymmetric across the dielectric core. (c) Calculated field profile due to a plane wave ($\lambda_0 = 450$ nm) incident on the metal dielectric waveguide array at normal incidence. The spatial field profile shown is composed of 15 repetitions of the unit cell. (d) Field profile due to a plane wave at an angle of incidence of 70° . Negative refraction is evident in the phase fronts, indicated by θ_i and θ_r . The scale bar in (c), (d) is 250 nm.

calculated analytically with the modal method, as described in the Appendix. The propagating mode is clearly not excited at all, but evanescent modes with exponentially decaying field profiles are visible near the interface. Since the propagating mode is not excited and the system is lossless, all power is reflected.

As mentioned in the Introduction, systems supporting only an antisymmetric propagating mode cannot be excited by a symmetric mode, such as a plane wave at normal incidence. In order to excite an antisymmetric mode, the symmetry of the incident wave has to be broken, which can be achieved by exciting the structure from an oblique angle of incidence. Figure 1(d) shows the calculated field distribution near the interface for a plane wave incident at 70° . Due to reflection at the interface an interference pattern is clearly observed in free space. However, for this geometry the propagating waveguide mode is also excited with a significant amplitude, as is visible in the bottom of the figure. Since the waveguide mode has a negative mode index, the wave fronts refract negatively. For an angle of incidence of $\theta_i = 70^\circ$, the waveguide mode index is $\beta_1^{(3)}/k_0 = -3.12$ ($k_0 = 2\pi/\lambda_0$), leading to a refraction angle of $\theta_r = -17.5^\circ$. Nevertheless, the high gradients of the mode field profile, as can be seen in Fig. 1(b), limit the excitation efficiency of this waveguide mode by a plane wave. As discussed above, at normal incidence the transmitted power $T = (\beta_2/\beta_1)|t_{12}|^2$ equals zero, where t_{12} is the complex transmission coefficient. At around an angle of 70° , transmission is maximum at approximately $T = 0.5$.

III. ANTIREFLECTION COATING DESIGN

A. Normal incidence

To improve transmission into the multilayer structure for arbitrary angles of incidence, we use a dielectric grating structure between the air half space and the waveguide array as an intermediate coupling layer that allows us to tailor the overlap between the incident field and the waveguide mode. A

general expression for the reflectivity of a two interface system is given by Airy's formula for reflection [27]:

$$r_{\text{total}} = \frac{r_{12} + r_{23} \exp(2i\beta_1^{(2)}d_2)}{1 + r_{12}r_{23} \exp(2i\beta_1^{(2)}d_2)}. \quad (1)$$

Here, $\beta_1^{(2)}$ is the propagation constant in region 2 (which now refers to the coating), and the subscripts ij on r refer to the reflection coefficient from medium i into medium j (i.e., r_{12} is the reflection coefficient from air to coating and r_{23} is the reflection coefficient from the interface between coating and metamaterial). From Eq. (1) it is clear that total destructive interference is achieved when $|r_{12}|$ and $|r_{23}|$ are equal in magnitude, and the thickness d_2 is properly chosen so that the two terms in the numerator are π out of phase [17]. For homogeneous planar media, this condition is satisfied when the coating has a quarter wavelength thickness and the refractive index equals $n_2 = \sqrt{n_1 n_3}$. In our case, however, an inhomogeneous geometry is required. Figure 2(a) shows a sketch of the proposed coupling layer geometry: a periodic multilayer with high-permittivity dielectric blocks with width

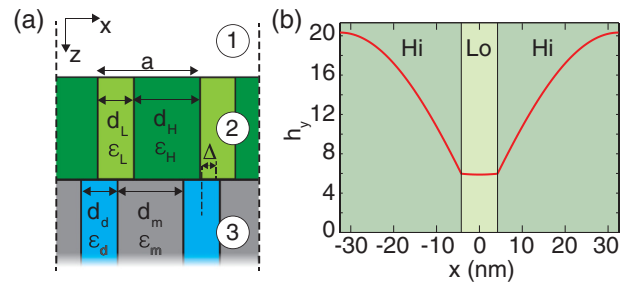


FIG. 2. (a) Sketch of the air/coupling layer/metal-dielectric metamaterial geometry. (b) Magnetic field profile of the propagating mode in the coupling layer with $\epsilon_{\text{Hi}} = 20.25$, $\epsilon_{\text{Lo}} = 1$, and $\rho_{\text{Hi}} = 0.87$, and a 65 nm unit cell size. The propagation constant of the eigenmode is $\beta_1^{(2)} = 43.85 \mu\text{m}^{-1}$.

d_{Hi} and permittivity ε_{Hi} , alternated with low-permittivity blocks with width d_{Lo} and permittivity ε_{Lo} in a unit cell with size a . If we match the unit cell size to the metamaterial, $a = 65$ nm, we find that for $\varepsilon_{\text{Hi}} = 20.25$ and $\varepsilon_{\text{Lo}} = 1$ there is only one propagating mode. This mode is symmetric, and as a result it can be efficiently excited from free space. By varying the filling fraction of the high-index dielectric ($\rho_{\text{Hi}} = d_{\text{Hi}}/a$), the reflectivity of the air/coupling layer interface can be controlled, which gradually changes from $R = 0$ when $\rho_{\text{Hi}} = 0$ to $R = 0.4$ as $\rho_{\text{Hi}} \rightarrow 1$ ($\varepsilon = 20.25$), where R is the reflected power ($R = |r_{12}|^2$). We take an air/coupling layer reflectivity of $R = 0.2$, which corresponds to a filling fraction $\rho_{\text{Hi}} = 0.87$. The field profile of the corresponding eigenmode is shown in Fig. 2(b) and has a propagation constant of $\beta_1^{(2)} = 43.85 \mu\text{m}^{-1}$.

The reflectivity of the coupling layer/metal-dielectric waveguide array interface may be controlled by displacing the coupling layer with respect to the metal-dielectric waveguide array. Such a displacement is necessary considering that the propagating mode in the coupling layer is still symmetric; as a result it cannot excite the antisymmetric mode if the unit cells of the two regions are symmetrically aligned. However, if we displace the coupling layer with respect to the substrate, this symmetry is broken, and the negative index waveguide mode can be excited. This displacement Δ is defined as the shift between the center of the low index layer of the dielectric grating and the center of the dielectric slab in the metal-dielectric array [see Fig. 2(a)]. The reflectivity of the coupling layer/metal-dielectric waveguide array interface is determined through numerical finite-difference time domain simulations (Lumerical FDTD 8.7.3) because the modal method does not converge well for this problem (see the Appendix for discussion). The results are shown in Fig. 3(a), where the reflectivity $|r_{23}|^2$ is plotted as a function of the displacement Δ . A small imaginary part of the dielectric constant of the metal ($\varepsilon_m = -3.5 + 0.01i$) was required for the stability of the simulations. This small amount of loss in the metal does not significantly affect the coupling process compared to the lossless system.

It is clear from Fig. 3(a) that the reflectivity is strongly modulated by the displacement, with reflections in the range of $|r_{23}|^2 = 0.1-1$. We observe particularly strong variations in reflection for a displacement between 5 and 7 nm, where the interface between the high and low index region of the dielectric grating crosses the metal/dielectric interface in the substrate. For $\Delta = 0$ nm and $\Delta = 32.5$ nm, the coupling layer is symmetrically oriented to the substrate, indeed preventing excitation of the antisymmetric mode.

For a displacement $\Delta = 7.8$ nm, the reflectivity $|r_{23}|^2 = 0.2$, which matches the reflectivity of the air/coupling layer interface. Then, in order to achieve full transmission of the incident wave to the metamaterial array, the thickness of the coating layer has to be tuned, such that the roundtrip phase pick up is π . Contrary to simple lossless homogeneous media, the phase shift upon reflection at the interfaces of the system under study generally will be different than 0 or π because energy is temporarily stored in evanescent fields close to the interfaces. Figure 3(b) shows the simulated reflectivity $|r_{\text{total}}|^2$ as a function of the coupling layer thickness. As expected, a clear periodic modulation of reflectivity is observed. Based

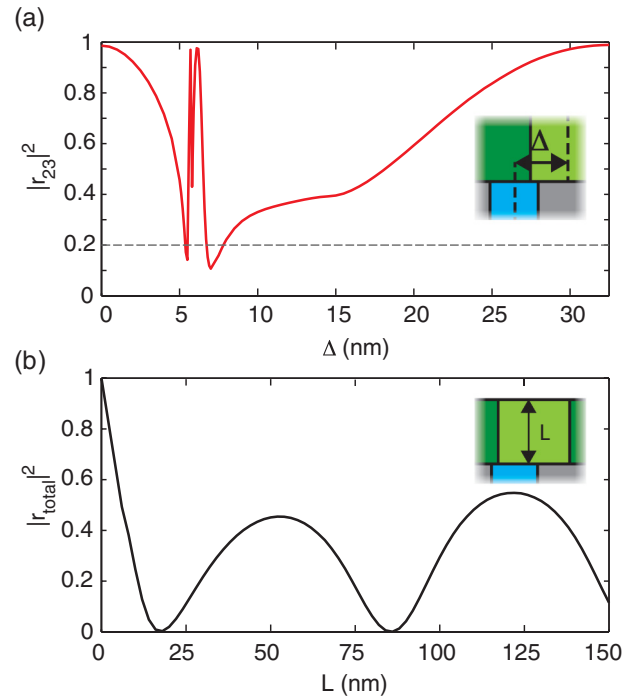


FIG. 3. (a) Simulated reflectivity (at $\lambda_0 = 450$ nm) of the coupling layer/waveguide array interface as a function of displacement Δ . The coupling layer is defined by $\varepsilon_{\text{Hi}} = 20.25$, $\varepsilon_{\text{Lo}} = 1$, and $\rho_{\text{Hi}} = 0.87$, and the unit cell size is $a = 65$ nm. The waveguide array is the same as in the above. (b) Simulated reflectivity of the combined coupling layer and waveguide array for $\Delta = 7.8$ nm with changing coupling layer thickness L . Clear oscillations are visible, corresponding to a standing wave in the coupling layer. The two local maxima in reflection are not equal in amplitude due to the influence of evanescent waves in the coupling layer.

on the propagation constant of the waveguide mode in the coating ($\beta_1^{(2)} = 43.85 \mu\text{m}^{-1}$), we expect a modulation period of $\pi/(\beta_1^{(2)}) = 72$ nm, which agrees well with Fig. 3(b). Because of the very small thickness of the coupling layer, the evanescent fields do not completely decay between the two interfaces, resulting in a different peak reflectivity for the two local maxima. For a coating layer thickness of $L = 86$ nm, a normally incident plane wave is completely transmitted to the antisymmetric mode of the metal-dielectric waveguide array. In contrast, without coupling layer this waveguide mode cannot be excited at all at normal incidence.

The complete transmission into the metal-dielectric waveguide array is clearly visible in Fig. 4(a), showing a normally incident plane wave coupling to the optimized geometry. The dashed lines indicate the locations of the interfaces. The incident field is visible above the coupling layer. The magnetic field distribution in the coupling layer shows a periodic modulation with maxima in the high-index dielectric, but it is clearly symmetric. In contrast, the field distribution in the metamaterial substrate is clearly antisymmetric. Due to the displacement of the symmetric field distribution in the coating with respect to the antisymmetric fields in the substrate, the symmetry constraint is relaxed, and efficient excitation of the antisymmetric mode is possible. By tuning the coating layer thickness, a condition can be found where

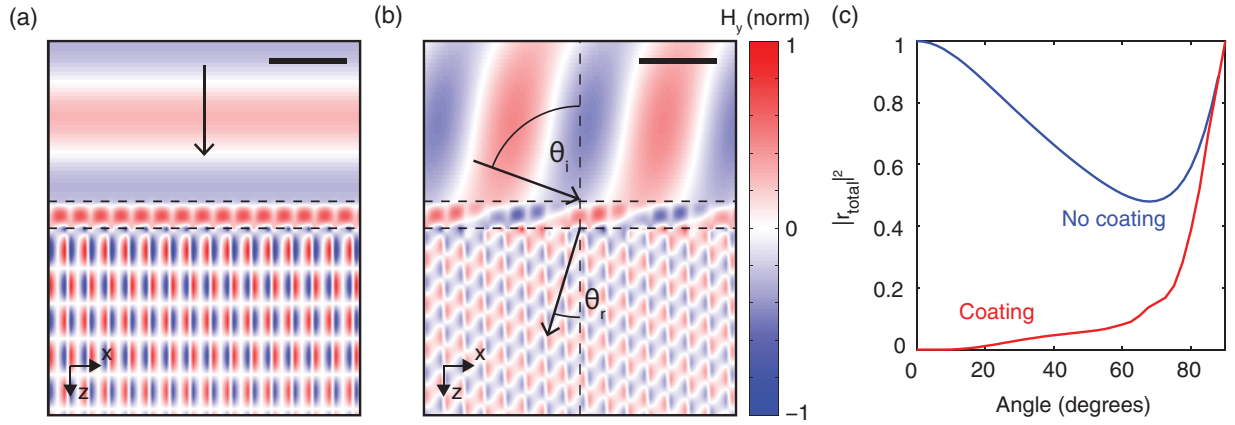


FIG. 4. (a) Simulated field profile at normal incidence. As is clear, the incident plane wave now very effectively couples to the antisymmetric waveguide mode. (b) Field profiles for a plane wave at an angle of incidence of 70° . The scale bar in (a), (b) is 250 nm. (c) Reflectivity from the total system as a function of angle of incidence (red). As a reference, the reflectivity of the bare multilayer substrate is also shown (blue).

destructive interference prevents any reflection, leading to perfect transmission.

B. Angle dependence

Just as with a regular antireflection coating, transmission remains large up to very high angles: Fig. 4(b) shows the magnetic field distribution for an angle of incidence of 70° , in which case 85% of the incident power is transmitted into the substrate. In fact, Fig. 4(c) shows that the reflectivity remains low for a large range of angles: $|r_{\text{total}}|^2 < 0.15$ for $\theta_i < 70^\circ$. In contrast, reflection off the bare waveguide array does not go below 50% and is minimum at 70° [Fig. 1(d)]. Interestingly, the reason for the low reflectivity over a broad angular range in the presence of the coupling layer is that the field overlap between the dielectric grating and the multilayer substrate is affected very little by changing the angle of incidence due to the subwavelength periodicity: The field profile in all layers experiences the same lateral phase gradient $\exp(ik_x x)$. On the other hand, the increase in reflectivity at oblique angles happens because the condition for destructive interference is no longer fulfilled due to (1) the angle dependence of the mode index, which changes the optical path length $\beta_1^{(2)} L$, and (2) the reflection coefficient of the first interface increases. These reasons also cause higher reflectivity at oblique angles in regular antireflection coatings.

While the proposed structure behaves very similarly to a regular antireflection coating in terms of the angle response, the frequency response will most likely be different. For homogeneous media, antireflection coatings typically operate over a broadband frequency range, given that material dispersion is limited (as is the case in, e.g., glass and silicon above 500 nm). Here, however, the reflectivity of the coating-metamaterial interface, may be expected to vary more strongly with frequency due to mode dispersion, thereby possibly limiting the operation bandwidth of the antireflection coating.

IV. DISCUSSION AND CONCLUSION

We have demonstrated that it is possible to achieve perfect transmission into the bulk metamaterial as long as a coating layer can be found that satisfies $|r_{12}| = |r_{23}|$. However, even

in the case that this condition is not satisfied, significant transmission enhancements can be achieved. This becomes evident if we look at the equation for minimum reflectivity R of such a multilayer system [27],

$$R_{\min} = \left| \frac{r_{12} - r_{23}}{1 + r_{12}r_{23}} \right|^2. \quad (2)$$

For example, it is possible that the coating/metamaterial interface remains very reflective ($r_{23} = 0.99$) due to extremely high field gradients that cannot be efficiently matched by the low field gradients in a dielectric coating layer. Even if the reflectivity of the air/coating interface is very low ($r_{12} = 0.20$, like glass), a total transmission of $1 - R_{\min} = 0.56$ is still achieved. Hence, even if perfect transmission is not attainable, significant transmission enhancements can still be achieved.

Finally, it is interesting to note that the two functions of the metamaterial antireflection coating (spatial engineering of the fields at the interface and tuning the propagation length to achieve destructive interference) do not necessarily require that the entire coating is inhomogeneous. For instance, one can also engineer the fields at the interface through, e.g., a plasmonic metasurface [28], which allows for strong field gradients, and use a homogeneous coating on top of the metasurface to achieve destructive interference. Such an approach may also be more straightforward to realize experimentally.

To conclude, we have proposed a method to enhance transmission from a plane wave into a planar complex metamaterial with a complex field profile. We achieve this by using an appropriately structured antireflection coating, which allows for efficient excitation of complex field profiles through spatial engineering of the field profile at the interface. In an example, we show that by optimizing the relative displacement between a coupling layer and a waveguide array and by changing the coupling layer thickness, even perfect transmission into the antisymmetric mode of the waveguide array can be achieved at normal incidence. High transmission is also observed for a broad range of angles: 100% at normal incidence and as high as 85% at 70° angle of incidence. Our results show that a thin metamaterial layer can be used as an efficient antireflection coating, enabling high transmission into structures with a

complex field profile. In this paper, we have shown how this may be applied to facilitate coupling to a waveguide array, but this approach may generally apply to any structure with a nonuniform field profiles, such as plasmonic waveguides, metamaterials with hyperbolic dispersion, epsilon-near-zero response, materials with an effective negative index response, and optical interconnects.

ACKNOWLEDGMENTS

We acknowledge Philippe Lalanne and Kokou Dossou for stimulating discussions. This paper is part of the research program of FOM, which is financially supported by The Netherlands Organization for Scientific Research (NWO). R.M. and A.P. were partially supported by the European Research Council with Grant No. 267634. D.S. and A.A. were partially supported by the Air Force Office of Scientific Research with Grant No. FA9550-13-1-0204. A.A. also acknowledges a fellowship of the Royal Netherlands Academy of Sciences (KNAW).

APPENDIX: THE MODAL METHOD AND CONVERGENCE

Here we describe the modal method used to numerically calculate the transmission and reflection from an interface between a homogeneous and a stratified medium or between two stratified media [29]. To calculate the reflection and transmission coefficients for inhomogeneous media, we need to expand the field in each region into its eigenmodes, $|\psi_n^{(j)}\rangle$. For propagation along z we have

$$\mathbf{H}^{(j)}(x, z) = H_0 \sum_{n=0}^{\infty} a_n e^{i\beta_n^{(j)} z} |\psi_n^{(j)}\rangle. \quad (\text{A1})$$

In Eq. (A1), the superscript refers to the region j , $\beta_n^{(j)}$ is the propagation constant of the n th eigenmode, and a_n is the corresponding complex amplitude. Using Ampere's law, we find for \mathbf{E} ,

$$\mathbf{E}^{(j)}(x, z) = E_0 \frac{i}{\varepsilon_j(x)} \sum_{n=0}^{\infty} a_n \beta_n^{(j)} e^{i\beta_n^{(j)} z} |\psi_n^{(j)}\rangle. \quad (\text{A2})$$

These eigenmodes in each region j are defined such that they are orthonormal under the pseudoinner product [30,31],

$$\begin{aligned} \langle \psi_m^{(j)} | \psi_n^{(j)} \rangle_{\varepsilon} &= \langle \psi_n^{(j)} | \frac{1}{\varepsilon_j(x)} | \psi_m^{(j)} \rangle \\ &= \int_{-a/2}^{a/2} \frac{1}{\varepsilon_j(x)} (h_{y,n}^{(j)}(x))^* h_{y,m}^{(j)}(x) dx = \delta_{nm}, \end{aligned} \quad (\text{A3})$$

where $\varepsilon_j(x)$ is the dielectric constant as a function of position and the asterisk denotes complex conjugation. Note that the pseudoinner product differs from the normal inner product because it includes $1/\varepsilon_j$ as a weighting function. In free space, the eigenmodes are simply plane wave harmonics for normal incidence $|\psi_n^{(j)}\rangle = \exp(in \frac{2\pi}{a} x) / \sqrt{a}$, where a is the periodicity. In the stratified medium, the expansion is performed using the waveguide modes of the geometry, which are found by solving the interface boundary conditions in a periodic unit cell [23,32]. Note that this orthonormality condition holds only for lossless systems, but that systems

with significant losses can also be treated analytically by applying the modal expansion method through an adjoint definition of the pseudoinner product [33].

The transmission and reflection amplitudes of a wave impinging on an interface at $z = 0$ can then be calculated by making use of the continuity of tangential fields [34],

$$\mathbf{H}^{(1)}(z = 0) \times \hat{\mathbf{n}} = \mathbf{H}^{(2)}(z = 0) \times \hat{\mathbf{n}}, \quad (\text{A4a})$$

$$\mathbf{E}^{(1)}(z = 0) \times \hat{\mathbf{n}} = \mathbf{E}^{(2)}(z = 0) \times \hat{\mathbf{n}}, \quad (\text{A4b})$$

where $\hat{\mathbf{n}}$ is the normal vector to the interface and the superscripts refer to the two half spaces. We find by substituting Eqs. (A1) and (A2) into the continuity Eqs. (A4a) and (A4b), the following equations:

$$\sum_{m=0}^{\infty} (a_m^+ + a_m^-) |\psi_m^{(1)}\rangle = \sum_{n=0}^{\infty} b_n^+ |\psi_n^{(2)}\rangle \quad (\text{A5a})$$

$$\frac{i}{\varepsilon_1(x)} \sum_{m=0}^{\infty} \beta_m^{(1)} (a_m^+ - a_m^-) |\psi_m^{(1)}\rangle = \frac{i}{\varepsilon_2(x)} \sum_{n=0}^{\infty} b_n^+ \beta_n^{(2)} |\psi_n^{(2)}\rangle. \quad (\text{A5b})$$

Here a_n and b_n are the mode amplitudes in medium 1 and 2 respectively, and the upper sign identifies forward and backward propagating amplitudes. Note that these equations are also valid for arbitrary angles of incidence, since the tangential fields for continuity are always given by Eqs. (A1) and (A2). Making use of the orthonormality condition in Eq. (A3), we can transform Eqs. (A5a) and (A5b) into coupled equations for the amplitudes a_m :

$$a_m^+ + a_m^- = \sum_{n=0}^{\infty} b_n^+ \langle \psi_m^{(1)} | \frac{1}{\varepsilon_1(x)} | \psi_n^{(2)} \rangle \quad (\text{A6a})$$

$$a_m^+ - a_m^- = \sum_{n=0}^{\infty} b_n^+ \frac{\beta_n^{(2)}}{\beta_m^{(1)}} \langle \psi_m^{(1)} | \frac{1}{\varepsilon_2(x)} | \psi_n^{(2)} \rangle. \quad (\text{A6b})$$

To solve this system numerically, we truncate the infinite series at a certain integer l , typically around 50. This leads to the matrix equation:

$$\begin{pmatrix} -\mathbf{I}_{l \times l} & \mathbf{B}_{m,n}^{(1)} \\ \mathbf{I}_{l \times l} & \mathbf{B}_{m,n}^{(2)} \end{pmatrix} \begin{pmatrix} \mathbf{a}^- \\ \mathbf{b}^+ \end{pmatrix} = \begin{pmatrix} \mathbf{a}^+ \\ \mathbf{a}^+ \end{pmatrix}, \quad (\text{A7})$$

where $\mathbf{I}_{l \times l}$ is the identity vector and the elements of the \mathbf{B} matrices are given by

$$B_{m,n}^{(1)} = \langle \psi_m^{(1)} | \frac{1}{\varepsilon_1(x)} | \psi_n^{(2)} \rangle \quad (\text{A8a})$$

$$B_{m,n}^{(2)} = \frac{\beta_n^{(2)}}{\beta_m^{(1)}} \langle \psi_m^{(1)} | \frac{1}{\varepsilon_2(x)} | \psi_n^{(2)} \rangle. \quad (\text{A8b})$$

The elements of \mathbf{a}^+ are known, as this is the incident field, given by a single plane wave. Such a linear system is easily solved numerically. We can relate these mode amplitudes to the reflection and transmission coefficients through $r_{12} = a^- / a^+$ and $t_{12} = b^+ / a^+$. In the case of the interface between free space and a stratified medium, these equations simplify to

$$B_{m,n}^{(1)} = \langle \psi_m^{(1)} | \psi_n^{(2)} \rangle \quad (\text{A9a})$$

$$B_{m,n}^{(2)} = \frac{\beta_n^{(2)}}{k_z^{(m)}} \langle \psi_m^{(1)} | \frac{1}{\varepsilon_2(x)} | \psi_n^{(2)} \rangle, \quad (\text{A9b})$$

where $k_z^{(m)}$ is the component of the free space wave vector along the z direction for the m th diffracted order. The free space eigenmodes are given by

$$|\psi_m^{(1)}\rangle = \exp\left(i\left(k_x + m\frac{2\pi}{a}\right)x\right). \quad (\text{A10})$$

In this case, the summation runs over negative indices as well, such that one sums from $m = -l/2$ to $m = l/2$ (for even l).

When solving for an interface between two stratified media, this formalism often shows very poor convergence. The reason is that due to the discontinuities in the permittivity, strong Gibbs oscillations arise in the finite expansions. When expanding two discontinuous bases on each other, as is essentially done in Eq. (A7), this leads to artificially large amplitudes for high harmonics. The rigorous coupled wave analysis formalism (RCWA) [or the Fourier modal method (FMM)], which is intricately related to the modal method [35], encountered similar convergence problems for TM polarization [36]. Convergence can be improved significantly by using a basis that is not affected by the discontinuities in ϵ , such as Gegenbauer polynomials [37].

-
- [1] D. R. Smith, P. Kolinko, and D. Schurig, Negative refraction in indefinite media, *J. Opt. Soc. Am. B* **21**, 1032 (2004).
- [2] V. M. Shalaev, Optical negative-index metamaterials, *Nat. Photon.* **1**, 41 (2007).
- [3] S. Dai, Q. Ma, T. Andersen, A. S. McLeod, Z. Fei, M. K. Liu, M. Wagner, K. Watanabe, T. Taniguchi, M. Thiemens, F. Keilmann, P. Jarillo-Herrero, M. M. Fogler, and D. N. Basov, Subdiffractive focusing and guiding of polaritonic rays in a natural hyperbolic material, *Nat. Commun.* **6**, 6963 (2015).
- [4] T. Tumkur, G. Zhu, P. Black, Y. A. Barnakov, C. E. Bonner, and M. A. Noginov, Control of spontaneous emission in a volume of functionalized hyperbolic metamaterial, *Appl. Phys. Lett.* **99**, 151115 (2011).
- [5] H. N. Krishnamoorthy, Z. Jacob, E. Narimanov, I. Kretzschmar, and V. M. Menon, Topological transitions in metamaterials, *Science* **336**, 205 (2012).
- [6] J. Kim, V. P. Drachev, Z. Jacob, G. V. Naik, A. Boltasseva, E. E. Narimanov, and V. M. Shalaev, Improving the radiative decay rate for dye molecules with hyperbolic metamaterials, *Opt. Express* **20**, 8100 (2012).
- [7] X. Yang, J. Yao, J. Rho, X. Yin, and X. Zhang, Experimental realization of three-dimensional indefinite cavities at the nanoscale with anomalous scaling laws, *Nat. Photon.* **6**, 450 (2012).
- [8] R. Maas, J. Parsons, N. Engheta, and A. Polman, Experimental realization of an epsilon-near-zero metamaterial at visible wavelengths, *Nat. Photon.* **7**, 907 (2013).
- [9] G. Shvets, Photonic approach to making a material with a negative index of refraction, *Phys. Rev. B* **67**, 035109 (2003).
- [10] X. Fan, G. P. Wang, J. C. W. Lee, and C. T. Chan, All-Angle Broadband Negative Refraction of Metal Waveguide Arrays in the Visible Range: Theoretical Analysis and Numerical Demonstration, *Phys. Rev. Lett.* **97**, 073901 (2006).
- [11] E. Verhagen, R. de Waele, L. Kuipers, and A. Polman, Three-Dimensional Negative Index of Refraction at Optical Frequencies by Coupling Plasmonic Waveguides, *Phys. Rev. Lett.* **105**, 223901 (2010).
- [12] R. Maas, E. Verhagen, J. Parsons, and A. Polman, Negative refractive index and higher-order harmonics in layered metal-dielectric optical metamaterials, *ACS Photonics* **1**, 670 (2014).
- [13] J. A. Dionne, E. Verhagen, A. Polman, and H. A. Atwater, Are negative index materials achievable with surface plasmon waveguides? A case study of three plasmonic geometries, *Opt. Express* **16**, 19001 (2008).
- [14] P. Spinelli, M. A. Verschuuren, and A. Polman, Broadband omnidirectional antireflection coating based on sub-wavelength surface Mie resonators, *Nat. Commun.* **3**, 692 (2012).
- [15] S. A. Mann, R. R. Grote, R. M. Osgood, and J. A. Schuller, Dielectric particle and void resonators for thin film solar cell textures, *Opt. Express* **19**, 25729 (2011).
- [16] J. van de Groep, P. Spinelli, and A. Polman, Single-step soft-imprinted large-area nanopatterned antireflection coating, *Nano Lett.* **15**, 4223 (2015).
- [17] K. X. Wang, Z. Yu, S. Sandhu, V. Liu, and S. Fan, Condition for perfect antireflection by optical resonance at material interface, *Optica* **1**, 388 (2014).
- [18] M. G. Moharam and T. K. Gaylord, Rigorous coupled-wave analysis of planar-grating diffraction, *J. Opt. Soc. Am.* **71**, 811 (1981).
- [19] P. Sheng, R. S. Stepleman, and P. N. Sanda, Exact eigenfunctions for square-wave gratings: Application to diffraction and surface-plasmon calculations, *Phys. Rev. B* **26**, 2907 (1982).
- [20] M. G. Moharam, T. K. Gaylord, E. B. Grann, and D. A. Pommet, Formulation for stable and efficient implementation of the rigorous coupled-wave analysis of binary gratings, *J. Opt. Soc. Am. A* **12**, 1068 (1995).
- [21] P. Lalanne and G. M. Morris, Highly improved convergence of the coupled-wave method for TM polarization, *J. Opt. Soc. Am. A* **13**, 779 (1996).
- [22] B. Sturman, E. Podivilov, and M. Gorkunov, Eigenmodes for metal-dielectric light-transmitting nanostructures, *Phys. Rev. B* **76**, 125104 (2007).
- [23] B. Sturman, E. Podivilov, and M. Gorkunov, Theory of extraordinary light transmission through arrays of subwavelength slits, *Phys. Rev. B* **77**, 075106 (2008).
- [24] T. W. Ebbesen, H. J. Lezec, H. F. Ghaemi, T. Thio, and P. A. Wolff, Extraordinary optical transmission through sub-wavelength hole arrays, *Nature* **391**, 667 (1998).
- [25] J. A. Porto, F. J. García-Vidal, and J. B. Pendry, Transmission Resonances on Metallic Gratings with Very Narrow Slits, *Phys. Rev. Lett.* **83**, 2845 (1999).
- [26] M. Foresti, L. Menez, and A. V. Tishchenko, Modal method in deep metal-dielectric gratings: the decisive role of hidden modes, *J. Opt. Soc. Am. A* **23**, 2501 (2006).
- [27] M. Born and E. Wolf, *Principles of Optics*, Vol. 1 (Pergamon Press, New York, 1964).

- [28] N. Yu and F. Capasso, Flat optics with designer metasurfaces, [Nat. Mater.](#) **13**, 139 (2014).
- [29] W. C. Chew, *Waves and Fields in Inhomogeneous Media*, Vol. 522 (IEEE Press, New York, 1995).
- [30] Ş. E. Kocabaş, G. Veronis, D. A. B. Miller, and S. Fan, Modal analysis and coupling in metal-insulator-metal waveguides, [Phys. Rev. B](#) **79**, 035120 (2009).
- [31] A. Zettl, *Sturm-Liouville Theory* (American Mathematical Society, Providence, Rhode Island, USA, 2010).
- [32] P. S. J. Russell, T. A. Birks, and F. D. Lloyd-Lucas, Photonic Bloch waves and photonic band gaps, in *Confined Electrons and Photons*, edited by E. Burstein and C. Weisbuch (Plenum Press, New York, 1995), pp. 585–633.
- [33] K. B. Dossou, L. C. Botten, A. A. Asatryan, B. C. P. Sturmberg, M. A. Byrne, C. G. Poulton, R. C. McPhedran, and C. M. de Sterke, Modal formulation for diffraction by absorbing photonic crystal slabs, [J. Opt. Soc. Am. A](#) **29**, 817 (2012).
- [34] J. D. Jackson, *Classical Electrodynamics*, 3rd. ed. (Wiley, New York, 1999).
- [35] P. S. J. Russell, Coupled wave versus modal theory in uniform dielectric gratings, [Opt. Commun.](#) **48**, 71 (1983).
- [36] L. Li, Use of Fourier series in the analysis of discontinuous periodic structures, [J. Opt. Soc. Am. A](#) **13**, 1870 (1996).
- [37] K. Edee, Modal method based on subsectional Gegenbauer polynomial expansion for lamellar gratings, [J. Opt. Soc. Am. A](#) **28**, 2006 (2011).